ELSEVIER

Contents lists available at ScienceDirect

Next Materials

journal homepage: www.sciencedirect.com/journal/next-materials



Research article



Development of pH indicator film containing butterfly pea flower (*Clitoria ternatea* L.) anthocyanin using locust bean gum/unbleached wheat flour matrix

Nur Nabilah Hasanah ^a, Ezzat Mohamad Azman ^a, Ashari Rozzamri ^a, Nur Hanani Zainal Abedin ^a, Mohammad Rashedi Ismail-Fitry ^{a,b,*}

- ^a Department of Food Technology, Faculty of Food Science and Technology, Universiti Putra Malaysia, 43400 UPM Serdang, Selangor, Malaysia
- ^b Halal Products Research Institute, Universiti Putra Malaysia, 43400 UPM Serdang, Selangor, Malaysia

ARTICLE INFO

Keywords: Butterfly pea flower Intelligent packaging Locust bean gum pH indicator Unbleached wheat flour

ABSTRACT

The growing interest in environmentally friendly packaging and smart food monitoring systems has driven the development of biodegradable films with pH-sensitive indicators. Among various biopolymers, natural gums and plant-based flours are being explored due to their film-forming abilities and biodegradability. In particular, locust bean gum (LBG) and unbleached wheat flour (UWF) exhibit potential due to their functional properties and abundance. This study aimed to determine the optimal film produced from LBG and UWF infused with anthocyanin from butterfly pea flower (BPF) extract, as a smart pH indicator. LBG's side branches can create a strong synergistic interaction with UWF, making it a promising matrix for producing pH indicator films. Films comprising 100 % LBG (L1), 100 % UWF (U1), 50 % LBG + 50 % UWF (LU), 70 % LBG + 30 % UWF (L2), and 30 % LBG + 70 % UWF (U2) were formulated. The physicochemical and microstructural characteristics of the different formulations were analysed. The pH indicator film containing 70 % LBG (L2) demonstrated greater stability, with lower moisture content (3.22 %), improved swelling properties (56.06 %), increased thickness (0.31 mm), strong water vapour permeability $(3.87 \times 10^{-6} \text{ g} \cdot \text{s}^{-1} \cdot \text{m}^{-1} \cdot \text{Pa}^{-1})$, high tensile strength (0.82 MPa), and good elongation at break (57.75 %) in comparison to the other films. Furthermore, the microstructural properties of L2 exhibited a compact and dense structure compared to the other films. L2 also displayed visible colour changes across various pH levels (1.0-13.0). In conclusion, L2 film demonstrated balanced characteristics, making it the most suitable film for selection as a pH indicator film with immobilised BPF anthocyanin, and proved its effectiveness as a freshness indicator when applied to silver pomfret samples.

1. Introduction

Rising consumer concerns about food safety and quality have driven interest in smart packaging, which provides real-time information on food freshness through active and intelligent functions [14,22,53,63]. pH indicator films, incorporating natural colourants like anthocyanins, change colour in response to volatile amines from bacterial activity, offering an efficient, low-cost, and non-toxic method for freshness monitoring [67]. Anthocyanins are vibrant, water-soluble pigments found in many plants, with colours ranging from blue to red depending on composition [6]. BPF (*Clitoria ternatea* L.) is a rich, stable source of anthocyanins—primarily ternatin and delphinidin—that produce an

intense deep blue colour [26,57].

Recent technologies for producing biodegradable packaging from renewable polymers or plant-based materials have emerged in response to environmental concerns regarding reliance on plastic packaging derived from petroleum. Polysaccharides, including gum, starch, and cellulose, have been utilised as components for future polymer alternative materials in film development [48]. LBG is a gum commonly regarded as a plant-derived heterogeneous polysaccharide, extracted using boiling water from the endosperm of the carob bean (*Ceratonia siliqua* L.) [68]. Due to LBG's excellent film-forming and biodegradable properties, it serves as a suitable matrix for the manufacture of packaging films [35]. Barak and Mudgil [8] reported that LBG's properties

E-mail address: ismailfitry@upm.edu.my (M.R. Ismail-Fitry).

^{*} Corresponding author at: Department of Food Technology, Faculty of Food Science and Technology, Universiti Putra Malaysia, 43400 UPM Serdang, Selangor, Malaysia.

consist of a β -(1 \rightarrow 4)-linked D-mannopyranosyl backbone with D-galactopyranosyl side branches attached via α -(l–6) linkage. LBG-based packaging films act not only as semi-permeable barriers to moisture and gases but also as carriers of bioactive substances, such as antibiotics, bacteriocins, plant extracts, and essential oils [35]. However, due to the high water uptake and low mechanical properties of single LBG films, they cannot be developed for practical application [58]. Yuan et al. [64] reported that the properties of LBG's D-galactopyranosyl side branches can create a strong synergistic interaction with other biopolymers such as polysaccharides, proteins, and lipids. Therefore, blending LBG with other substances, including biopolymers, hydrophobic compounds, and plasticisers, presents a viable approach to counteracting the limitations of films made solely from LBG.

UWF provides a denser structure and acts as a structure-building agent due to the interaction between gluten and starch content [34]. In conjunction with that, UWF might be suitable as a complementary material for LBG films. UWF and bleached wheat flour (commercial) have little difference. Bleached flour typically has a higher pH due to the use of alkaline bleaching agents like chlorine [41], resulting in a slightly more alkaline pH and potentially interfering with pH-sensitive components in films [42] compared to UWF. UWF generally has a pH between 6.0 and 6.8, making it slightly acidic but closer to neutral. UWF, with its denser texture, off-white colour, and natural chemical composition, was selected for developing pH indicator films to avoid bleaching agents that may affect pH sensitivity [7]. Its slightly acidic pH could enhance interaction with pH-sensitive dyes, though no specific studies on its use in such films have been reported.

In conjunction with that, five different LBG/UWF ratios (100:0, 70:30, 50:50, 30:70, and 0:100) were selected to systematically evaluate the effects of varying gum-to-flour proportions on the films' functional and structural properties, and to identify the most suitable combination for pH indicator applications. LBG has high water uptake, which can limit film performance. Blending it with UWF in different proportions allows variation in water absorption and other characteristics, enabling optimisation of the final film formulation. Therefore, this study aimed to develop five LBG/UWF film formulations incorporating BPF anthocyanin and to evaluate their structural, physical, and functional properties for potential use as biodegradable intelligent packaging.

2. Methodology

2.1. Materials

Fresh BPF were purchased from a local farmer (Shah Alam, Selangor, Malaysia). LBG and UWF were obtained from Mei Loon Sdn. Bhd, Selangor, Malaysia. All chemicals used, such as ethanol, hydrochloric acid (HCl), sodium hydroxide (NaOH), potassium dihydrogen phosphate anhydrous (KH $_2$ PO $_4$), potassium hydrogen phthalate (C $_8$ H $_5$ KO $_4$), sodium carbonate (NaCO $_3$), and borax, were supplied from Scienfield Expertise PLT, Selangor, Malaysia.

2.2. Extraction of BPF anthocyanin

The petals of BPF were removed from the stem and leaves, and then dried using a freeze-dryer (FreeZone 4.5, Labconco, USA) at $-48^{\circ}\mathrm{C}$ for 48 h to preserve the anthocyanin content. After that, the dried BPF was ground into a powder form using a dry mill (MX-EX1031, Panasonic, Malaysia) and then passed through a 0.841 mm (20 mesh) sieve. Exactly 2.5 g of BPF powder was dissolved in 100 mL of 50 % (v/v) ethanol and sonicated using a probe ultrasonicator (Q500, QSonica Sonicator, USA) for 25 min at 60 % amplitude and 240 V. This method followed according to Santos, Martins [49] with slight modifications. The extracts were filtered using a vacuum filter to remove the solid residues. The BPF extracts were covered with aluminium foil and stored in the freezer at $-20^{\circ}\mathrm{C}$ before further analysis.

2.3. Formulation of the pH indicator films

The film preparation method, as described by Li et al. [34], was used with some modifications. The solvent casting method was used to prepare the pH indicator films. The LBG solution was prepared by dissolving 2 g of LBG in 100 mL of distilled water (2 % w/v) and stirring at 80°C for 30 min using a magnetic stirrer (MS-H280-Pro, DLAB Scientific Inc., Malaysia) until complete gelation was achieved. The UWF solution was prepared by dissolving 4 g of UWF in 100 mL of distilled water (4 % w/v), followed by the addition of 30 % glycerol into the solution. The two polymer solutions were mixed in the following proportions: LBG: UWF 100:0 (L1), 0:100 (U1), 50:50 (LU), 70:30 (L2), and 30:70 (U2). After that, the solution was cooled to 40°C, and 3 mL of BPF anthocyanin extract was added, followed by thorough mixing for 15 min. The solution was then sonicated for 10 min at 30°C to remove the air bubbles, and the film-forming solution (30 mL) was poured into a petri dish (diameter of 140 mm). The films were dried in a hot air dryer oven (ED 23, Dynamic Oven Binder, Germany) at 40°C for 18 h. The dried films were peeled and kept in a desiccator until the evaluation.

2.4. Determination of the physical properties of pH indicator film

2.4.1. Film thickness

The thickness of the films was measured at five random points on each film by using a hand-held digital micrometre (C112XBS, Mitutoyo, Japan) with an accuracy of 0.001 mm. The average values were calculated [39].

2.4.2. Moisture content

The moisture content of films was determined by using a moisture analyser (MX-50, A&D, Japan). The film was cut into a square shape (4 \times 4 cm) and dried until a constant weight of the film was achieved. The percentage of moisture was recorded and analysed.

2.4.3. Swelling properties

Swelling properties were determined by cutting film samples into a square shape (2 cm \times 2 cm) and drying in an oven at 60°C for 24 h [4] with slight modification. The dried film was weighed (W₀) and then immersed in a beaker containing 20 mL of distilled water for 24 h. The surface of the swollen film was blotted with filter paper to remove any adsorbed water before being weighed again (W₁) and calculated according to Eq. (1):

$$\%Swelling = \frac{W_1 - W_0}{W_1} \times 100 \tag{1}$$

2.4.4. Water solubility

The solubility test was analysed according to the method of Hanani et al. [25] with slight modifications. A film sample (2 cm \times 2 cm) was cut from a different formulation, dried at $105^{\circ}C$ for 24 h by oven-drying, and weighed to determine the initial dry weight (W_0). After that, the dried films were immersed in 50 mL of distilled water for 24 h. The residual pieces of film were taken out and re-dried at $105^{\circ}C$ overnight. The weight percentage of the total soluble matter of the final films (W_1) was calculated using the following Eq. (2):

$$\%Solubility = \frac{W_0 - W_1}{W_0} \times 100 \tag{2}$$

2.4.5. Water vapour permeability (WVP)

The WVP of the film was analysed gravimetrically according to the method of Adilah et al. [3]. Briefly, the film sample was sealed over 30 mL of a crucible containing 6 mL of distilled water. Afterwards, the crucible was maintained at $23 \pm 2^{\circ} \text{C}$ and 50 ± 5 % relative humidity (RH) in a desiccator containing silica gel. The crucible was left for 8 h, and the weight difference was monitored at 1 h intervals. WVP of the film was determined by the following Eq. (3):

$$WVP = \frac{\Delta w \times l}{A \times t \times P}$$
 (3)

Where Δw is the weight difference (g); l is the film thickness (m); A is the exposed area of the film (m²); t is the time (s); and P is the partial pressure difference of water vapour (Pa).

2.4.6. Mechanical properties

The mechanical analysis of films was evaluated using a method developed by Xue et al. [60] with a texture analyser (TA.XT2i, Stable Micro Systems, UK). Film samples were cut into rectangular strips (3 cm \times 6 cm) and fitted between the tight-grip and using the A/TG system tensile mode. The parameters used were: a minimum induction force of 5 g, a pre-test speed of 1 mm/s, a test speed of 1 mm/s, and a post-test speed of 3 mm/s. The tensile strength (TS) and elongation at break (EB) were calculated based on the following Eqs. (4) and (5):

$$TS = \frac{F}{S} \tag{4}$$

$$EB = \frac{(L - L_0)}{L_0} \times 100$$
 (5)

Where F is the maximum tension of film at fracture (N); S is the cross-sectional area (mm 2); L is the final length (mm); and L $_0$ is the initial length (mm).

2.4.7. Appearance and colour analysis

The film's appearance was captured using a digital camera against a white background. The colour analysis of the film was conducted with a colourimeter (CR-410, Chroma Meter, Japan), based on three colour coordinates: L*, a*, and b*. The colour was measured using the units L* (Lightness/darkness; 0–100), a* (positive = redness/negative = greenness), and b* (positive = yellowness/negative = blueness).

2.5. Structural characterisation of pH indicator film

2.5.1. Scanning electron microscopy (SEM)

Scanning Electron Microscope (SEM) analyses were performed according to Peralta et al. [45] with slight modifications. The film samples were immersed in cryogenic fracture and cut into a square strip (2 cm \times 2 cm). After that, the samples were sputter-coated with gold and attached to the aluminium tape stub. The micrographs of the surface and cross-section of the films were observed using scanning electron microscopy (JEOL, JSM-5800LV, Japan) using operational conditions: voltage $=5~\rm kV$ and magnification $=500~\rm \times$.

2.5.2. Fourier transform infrared spectroscopy (FTIR)

The chemical structure of the films was examined using an attenuated total reflection-Fourier transform infrared (ATR-FTIR) spectrometer (1760X, PerkinElmer, USA) to investigate the relationship between the sample materials and their film-forming properties. Absorbance spectra of films were obtained from 4000 to 400 cm $^{-1}$ [27].

2.6. Colour response of L2 film indicator to different pH values (1.0-13.0)

To evaluate the colour sensitivity of the film samples to changes in pH, the films were cut into a square shape $(4 \text{ cm} \times 4 \text{ cm})$ and then immersed in solutions with different pH values. The pH solutions were prepared using 1 M HCl (pH 1.0, 2.0, 3.0, 4.0, 5.0, and 6.0) and 1 M NaOH (pH 7.0, 8.0, 9.0, 10.0, 11.0, 12.0 and 13.0). The colour changes of the films were recorded by a digital camera with a white background.

2.7. Colour stability and light barrier properties of L2 film during storage

The storage analysis of the film was analysed according to the

method of Chen et al. [15] with slight modifications. The L2 film indicator was stored for 9 days at three different temperatures: (1) room temperature (25°C); (2) chilled temperature (4°C); and (3) frozen temperature (-18°C). The colour changes of the indicator were assessed every 3 days, and total colour difference (ΔE) and opacity of the film were calculated.

2.8. Application of L2 film to monitor the freshness of the fish

The L2 films were used to monitor the freshness of silver pomfret fish. The films were cut into squares (3 cm \times 3 cm) and attached to the lid of the containers (10 cm \times 10 cm \times 4.5 cm). Each container contained approximately 30 g of sample weight and was stored in a chiller (4 \pm 1 °C) for 6 days, and was analysed every 48 h. The fish sample was evaluated for their pH values and colour appearance by the naked eye. For pH measurements, the sample was homogenised with distilled water for 5 min using a homogeniser (Heidolph Silent Crusher, Schwabach, Germany). Whereas the colour changes of the pH indicator film were evaluated using a chromameter [30].

2.9. Statistical analysis

All analyses were performed in triplicate. Statistical analysis for all data was conducted using MINITAB Statistical Software (MiniTab Inc., USA). One-way analysis of variance (ANOVA) was performed, and Tukey's tests at a 95 % confidence level (p < 0.05). The results obtained in this research were expressed as the mean values \pm standard deviation.

3. Results and discussion

3.1. Physical properties of pH indicator film

3.1.1. Film thickness

Thickness is a crucial factor in creating packaging film as it affects opacity, sturdiness, and water vapour permeability [13]. Based on Table 1, the thickness of films ranged from 0.16 to 0.39 mm, with U1 films being the thickest at 0.39 mm (p > 0.05) and L1 films being the thinnest at 0.16 mm (p < 0.05). Blended films of LBG and UWF in different ratios (LU, U1 and U2) exhibited significantly thicker films compared to 100 % LBG (L1). This can be attributed to the differences in composition, molecular structure, crystallinity, and the process of gel

Table 1The physical properties of the pH indicator film with different ratios of LBG and UWF incorporated with BPF anthocyanin.

		-				
Physical	Film types					
Properties	L1	U1	LU	L2	U2	
Thickness (mm)	$\begin{array}{l} 0.16 \\ \pm \ 0.02^b \end{array}$	$\begin{array}{l} 0.39 \\ \pm \ 0.12^a \end{array}$	$\begin{array}{l} 0.35 \\ \pm \ 0.04^a \end{array}$	$\begin{array}{l} 0.31 \\ \pm \ 0.03^a \end{array}$	$\begin{array}{l} 0.39 \\ \pm \ 0.08^a \end{array}$	
Moisture Content (%)	$\begin{matrix}3.79\\\pm2.19^b\end{matrix}$	$\begin{array}{l} 9.58 \\ \pm \ 2.69^a \end{array}$	$\begin{array}{l} 4.26 \\ \pm \ 1.91^b \end{array}$	$\begin{matrix}3.22\\\pm 1.72^{b}\end{matrix}$	$\begin{matrix} 6.85 \\ \pm \ 2.59^{ab} \end{matrix}$	
Swelling power (%)	$\begin{array}{l} 94.28 \\ \pm \ 2.81^a \end{array}$	$\begin{matrix}22.55\\ \pm 11.43^{d}\end{matrix}$	$67.43 \\ \pm 6.97^{bc}$	56.06 ± 1.53^{c}	$75.61 \\ \pm 3.18^{\mathrm{b}}$	
Water Solubility (%)	$\begin{array}{l} 80.03 \\ \pm \ 4.08^a \end{array}$	20.79 ± 5.71^{c}	$\begin{array}{l} 81.77 \\ \pm \ 6.70^a \end{array}$	$\begin{array}{l} 40.02 \\ \pm \ 12.95^{bc} \end{array}$	$\begin{matrix}62.01\\\pm 8.92^{ab}\end{matrix}$	
Water Vapour Permeability (x 10^{-6} g. $s^{-1}m^{-1}Pa^{-1}$)	$\begin{array}{l} 2.80 \\ \pm \ 0.23^a \end{array}$	$1.15 \\ \pm 1.08^a$	$\begin{array}{l} 2.31 \\ \pm 1.34^{a} \end{array}$	$\begin{array}{l} 3.87 \\ \pm \ 0.62^a \end{array}$	5.59 ± 1.57^{a}	
Tensile strength (MPa) Elongation at break (%)	$\begin{array}{l} 0.83 \\ \pm \ 0.15^a \\ 37.13 \\ \pm \ 4.66^b \end{array}$	$egin{array}{l} 0.01 \ \pm 0.01^{ m b} \ 67.43 \ \pm 3.84^{ m a} \end{array}$	$\begin{array}{l} 0.09 \\ \pm \ 0.02^b \\ 60.20 \\ \pm \ 8.28^a \end{array}$	$\begin{array}{l} 0.80 \\ \pm \ 0.12^a \\ 53.75 \\ \pm \ 11.63^{ab} \end{array}$	$egin{array}{l} 0.07 \ \pm \ 0.08^b \ 61.86 \ \pm \ 4.23^a \end{array}$	

All values are mean \pm standard deviation of three replicates. Means that do not share the same letter are significantly different (p<0.05) in the same row. L1 = 100 LBG:0 UWF; U1 = 0 LBG: 100 UWF; LU= 50 LBG: 50 UWF; L2 = 70 LBG: 30 UWF; U2 = 30 LBG: 70 UWF.

formation of LBG and UWF, as outlined in Table 2 [54,68,8,37,24]. LBG film (L1) was thinner than UWF (U1) because the amorphous structure of LBG allowed better solubility of the polymer in water [52]. This resulted in a more homogeneous film-forming solution, which in turn produces a more ordered structure and consequently forms compact and thinner films. Yong et al. [62] reported similar findings, where LBG produced thinner films when blended with other starch-based films. In contrast, UWF-dominant films were thicker due to the semi-crystalline structure of the starch-dominant UWF, which reduces the solubility of UWF in water [24]. This led to a less ordered structure, resulting in thicker films. Blended films exhibited an intermediate thickness between L1 and U1, indicating that the mixture of LBG and UWF enhances the solubility of the film-forming solution and produces a more homogeneously dispersed polymer matrix compared to 100 % UWF (U1).

3.1.2. Moisture content

Moisture content is a crucial factor for food packaging materials because high moisture levels can encourage the growth of microbes on the surface of packaged foods [16]. Based on Table 1, there was a significant difference (p < 0.05) in U1, which has the highest moisture (> 10 %), so it was considered unsuitable for creating a pH indicator film. This is attributed to the presence of gluten in UWF, which has a good water absorption capacity and can form a three-dimensional network structure after hydration, retaining water in the film even after drying [21]. In contrast, L2 has the lowest moisture content (3.22 %) and the thickest film (0.31 mm), indicating the homogeneity of the film compared to other formulations.

3.1.3. Swelling properties

The swelling property was defined as the water uptake percentage of the film until saturation was reached, and the swelling behaviour was proportional to the total water molecules contained in the polymer

Table 2Comparison of composition, molecular structure, crystallinity and gel formation of locust bean gum (LBG) and unbleached wheat flour (UWF).

Properties	LBG	UWF
Composition	Contains approximately 80–85 % galactomannan (of which 50–65 % is mannose, 14–18 % is galactose, and the rest are traces of glucose, rhamnose, arabinose and xylose), 10–12 % moisture, 5 % protein, 1.0 % ash, 1.0 % crude fibre, 0.5 % fat.	Mainly contains a combination of starch (78–82 %) and protein (8–16 %).
Molecular structure	A non-starch polysaccharide composed of β -(1 \rightarrow 4)- linked D-mannopyranosyl backbone with D-galactopyranosyl side branches attached via α -(1–6) linkage	The starch is made up of amylose (linear structure and bonded via 1,4-α-glycosidic linkage) and amylopectin (branched structure linked via 1,6-α-glycosidic bond).
Crystallinity	Amorphous LBG hydrates easily due to its amorphous structure, forming a gel-like network.	The starch has a semi- crystalline structure composed of alternating amorphous regions (predominantly amylose) and crystalline regions (mainly amylopectin). Crystalline regions act as barriers to water absorption making it less soluble in cold water.
Formation of gel	Gelation through thermal hydration	Gelatinisation (the process of heating starch in excess water, melting of starch crystallites, and the granules lose their molecular order, structure, and birefringent character, and simultaneously starch solubilization takes place)

matrix of the film [31]. The greater the water uptake, the greater the swelling property. Based on Table 1, there was a significant difference in swelling power among all films, with L1 exhibiting the highest swelling power (94.28 %) and U1 showing the lowest (22.55 %). The high swelling power of L1 is attributed to its amorphous structure, which facilitates interaction and penetration of water molecules into the polysaccharide chains, resulting in the formation of a swollen gel. Conversely, U1 demonstrated the lowest swelling ability (p < 0.05) due to its semi-crystalline structure, which resists water penetration and limits swelling capability.

Furthermore, the properties of amylose act as a swelling inhibitor [28]. The low swelling rate was potentially due to intermolecular interactions between the linear chain of amylose starch and the BPF extract, which inhibited starch swelling and allowed for less water uptake in the polymer matrix [66]. Ahmad et al. [4] reported similar findings, where sago starch film was less affected and swelled significantly less compared to other starch films. On the other hand, the blended films exhibit intermediate swelling power (56.06–75.61 %), indicating a synergistic effect stemming from the combination of LBG and UWF. In these films, LBG disrupts the crystalline regions of UWF, enhancing the water uptake capacity of the composite films. The amorphous nature of LBG creates more water-accessible regions, contributing to the improved swelling behaviour of the blended films.

3.1.4. Water solubility

In film fabrication, water solubility is a vital attribute to consider, as it indicates the water resistance ability and integrity of polysaccharide films (Atef, Rezaei, & Behrooz, 2014). Generally, higher water solubility is not desirable for developing food packaging due to its limitations for foods in high relative humidity environments. Similarly, in line with its swelling properties, U1 displays significantly lower water solubility (p < 0.05) compared to L1 and the blended films (Table 1). This is primarily because a substantial portion of the starch in U1 maintains its semi-crystalline structure, which restricts water interaction and reduces solubility. In contrast, LBG exhibits high water solubility due to its amorphous structure, which facilitates extensive interaction with water and allows for easy hydration. The blended mixture of LBG and UWF balances these properties, resulting in films with moderate solubility. Among the blended films, L2 demonstrated the lowest water solubility, making it suitable for a wide range of applications. These findings regarding swelling and water solubility further support the selection of LBG/UWF as the polymer blend for developing pH indicator films.

3.1.5. Water vapour permeability (WVP)

WVP is a crucial factor in determining the moisture transfer of polymeric materials in intelligent packaging film performances, which protects and prolongs the shelf life of food products. Based on Table 1, there is no significant difference among all films (p < 0.05). Theoretically, based on the results of swelling power and water solubility, LBG was expected to have lower water resistance properties (high WVP) due to its high water affinity resulting from its amorphous structure. In contrast, UWF was expected to have better water resistance and, therefore, a lower WVP, as suggested by previous findings (swelling power and water solubility). However, WVP is primarily influenced by the structural characteristics of the films, such as the formation of ordered structure, the presence of voids, or tortuous pathways caused by dispersed particles such as BPF extract [36,40] to prevent moisture transfer through the film, on top of its water affinity properties as discussed in previous analyses (swelling power and water solubility). In L1, the homogeneous film-forming structure facilitates the development of a more ordered and compact matrix, which effectively reduces moisture transfer, resulting in a lower water vapour permeability (WVP) [38], despite its high swelling power and water solubility. On the other hand, the insoluble crystalline regions in U1 disrupt the formation of an ordered structure, creating voids that allow moisture to pass through, thus causing high WVP. In blended films, both properties were adjusted,

resulting in an intermediate WVP. Similar findings were reported by Hashim et al. [27], who investigated the WVP values of different formulations of sugarcane wax and agar, showing that there were no significant differences in WVP values.

3.1.6. Mechanical properties

Table 1 presents the mechanical properties of the pH indicator film, comprising different ratios of LBG and UWF, expressed as tensile strength (TS) and elongation at break (EB). TS is defined as the maximum tolerance of the composite films against the applied stress when being pulled or stretched before breaking occurs. Moreover, EB is defined as the maximum capability of composite films to maintain alterations in their length and shape without any crack formation [1]. Based on Table 1, LBG-dominant films (L1 and L2) exhibited the highest TS, with a significant difference (p < 0.05) compared to the other films. This is because the amorphous structure allows LBG to form homogeneous film-forming solutions and produce films with compact, dense and ordered structures [43]. This provided films with higher rigidity, thus increasing the tensile strength. Additionally, due to the presence of abundant hydroxyl groups, LBG can form strong synergistic interactions between the D-galactopyranosyl side branches and other biopolymers (UWF) through hydrogen bonds [64]. In contrast, UWF films (U1, LU, and U2) showed significantly lower tensile strength compared to LBG dominant films. The low tensile strength of UWF dominant films is attributed to the less ordered structure resulting from the insoluble crystalline regions. This disrupts the formation of a more rigid matrix, thus lowering the tensile strength.

In terms of EB, UWF dominant films (U1, LU, and U2) exhibited significantly higher EB compared to LBG films, showing an opposite trend to that of tensile strength (TS). This is due to the significantly higher moisture content of UWF films that act as a lubricant to improve the flexibility of the film, thus increasing the EB [59]. Furthermore, these results appear to be linked to the amylose/amylopectin and protein (gluten) content of UWF [20]. UWF films contain gluten (made up of glutenin and gliadin). Glutenin forms a distinctive protein network through disulfide bonds, providing cohesiveness and elasticity to the film. Meanwhile, gliadin acts as a plasticiser within this protein network, enhancing the ductility of UWF films [21]. Collectively, these interactions improved the EB of UWF films. The U1 and U2 films consist of high concentrations of amylose and amylopectin, which provide adequate polymer linear chain motion and allow chain-chain connections of polymeric backbones by hydrogen bonds [28]. Although L2 slightly decreases the percentage of EB, it maintains a stable film in terms of TS mechanical properties, as evidenced by the uniform and compact morphology structure of L2, as observed through SEM (Table 4). Similarly, the result is supported by Mostafavi et al. [43]. This demonstrated that LBG can be combined with polysaccharides to enhance the mechanical properties of the film.

3.1.7. Film appearance and colour analysis

Based on Table 3, the inclusion of BPF anthocyanin influenced the appearance and blue colour of the surface-intelligent pH indicator film. All film samples exhibited a blue colour because of the delphinidin anthocyanin that is responsible for the deep blue to purple colour of BPF [11]. Apart from that, there was no significant difference between all types of film (p>0.05) in lightness (L*), which can be attributed to the white colour properties of the LBG and UWF powder. Additionally, the redness (a*) was not affected since the anthocyanin concentration used in the film formulation was fixed. These results indicate an excellent dispersion between anthocyanin and polymer matrix, which did not affect the pH indicator film's colour properties.

3.2. Structural characterisation of pH indicator film

3.2.1. Fourier transform infrared spectroscopy

The FTIR-identified differences between the molecular interactions

Table 3Appearance and colour of the pH indicator film with different ratios of LBG and UWF incorporated with BPF anthocyanin.

Film	Appearance	Lightness (L*)	Redness (a*)	Yellowness (b*)
L1		$57.26 \\ \pm 1.35^a$	$5.12 \\ \pm 0.47^a$	-20.01 ± 0.58^{c}
U1		$58.18 \\ \pm 1.72^a$	$\begin{array}{l} 3.85 \\ \pm \ 0.51^a \end{array}$	-12.51 ± 1.67^{a}
LU		$50.35 \\ \pm \ 2.11^a$	$\begin{array}{l} 6.23 \\ \pm \ 0.95^a \end{array}$	$-18.30 \\ \pm 1.12^{bc}$
L2		57.06 ± 7.98^{a}	$\begin{array}{l} 6.03 \\ \pm \ 1.82^a \end{array}$	$-15.47 \\ \pm 2.58^{ab}$
U2		$\begin{array}{l} 59.31 \\ \pm \ 1.97^a \end{array}$	$\begin{array}{l} 4.12 \\ \pm 0.38^{a} \end{array}$	$-14.90 \\ \pm 0.48^{ab}$

All values are mean \pm standard deviation of three replicates. Means that do not share the same letter are significantly different (p<0.05) in the same column. L1 = 100 LBG:0 UWF; U1 = 0 LBG: 100 UWF; LU= 50 LBG: 50 UWF; L2 = 70 LBG: 30 UWF; U2 = 30 LBG: 70 UWF.

and chemical structure of pH indicator films are observed in Fig. 1. All the film's samples with anthocyanin displayed a dominant band at 3281–3331 cm⁻¹, where N-H/O-H stretching and 2923–2934 cm⁻¹ for C-H stretching vibrations, which corresponds to the aliphatic moieties in polysaccharides [23]. Additionally, the formation of hydrogen bonds between the BPF anthocyanin and the film matrices also contributed to this effect. Apart from that, L1 and L2 exhibited a typical band at 811 cm⁻¹, corresponding to the mannose residues of LBG [65]. The wavenumber in the range 1651–1654 cm⁻¹ corresponds to the Amide I band, which is associated with the C=O stretching vibration and can be used to distinguish α - and β -gliadins [55] of the secondary structure protein (gluten) in the film. The peaks at 2882 cm⁻¹ and 2884 cm⁻¹ confirmed the presence of hydrogen bonding in the BPF anthocyanin extract, which is assigned as O-H stretching [18]. Wavenumber 1026–1022 cm⁻¹ reflects the degree of double-helix structure in starch granules [29], where a similar report was made on saccharide structure between 1035 and 1023 cm⁻¹ in different polysaccharide/PVA films incorporated with red pitaya betacyanin [61]. All of the film samples had similar diffraction spectra, indicating that the addition of LBG and UWF at any concentration did not affect the functional group of the intelligent pH BPF indicator film.

3.2.2. Scanning electron microscopy

The microstructures of pH-intelligent films with different compositions of LBG and UWF are shown in Table 4. LBG-dominated films (L1 and L2) showed a relatively smooth structure due to the high homogeneity of LBG in the film-forming solution. Meanwhile, UWF-dominated films (U1 and U2) and also LU films had a rough surface, indicating that starch globules were not well dispersed in the polymer matrix, probably due to the semi-crystalline structure of starch, which has low solubility in water.

Additionally, the high polymer content in the film causes it to become saturated with starch granules, resulting in incomplete polymer gelatinisation [4]. Among all films, L2 has a compact and dense structure, with no pores visible in the cross-sectional view. A similar

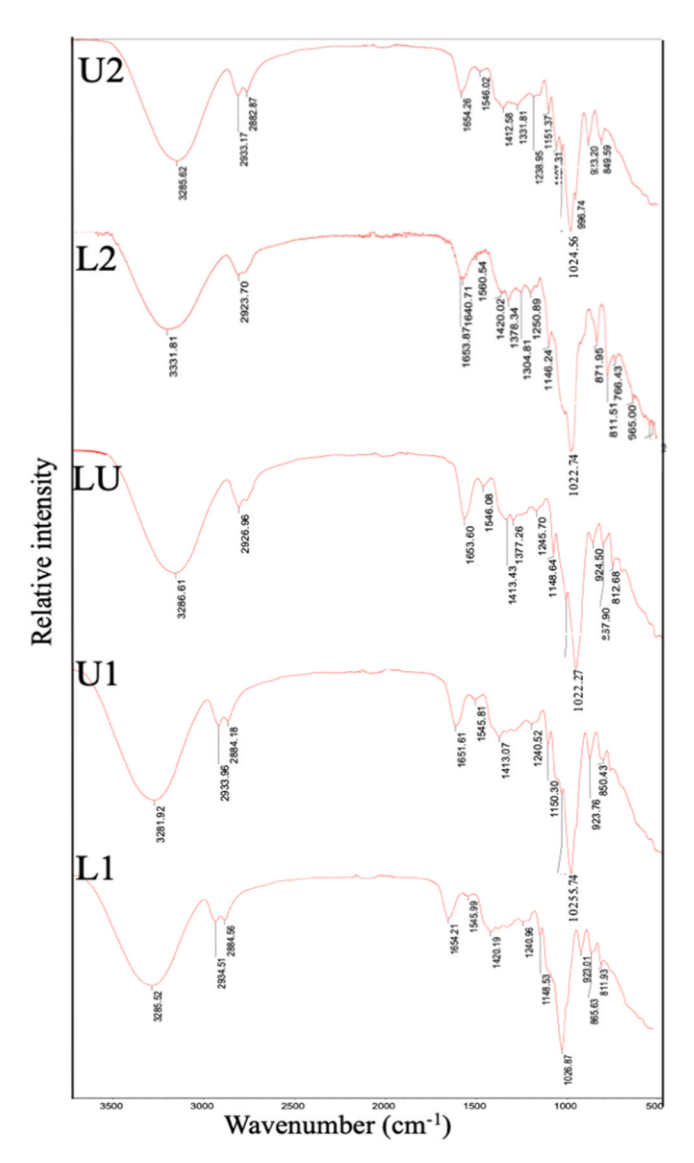


Fig. 1. FTIR spectra of the pH indicator film with different ratios of LBG and UWF incorporated with BPF anthocyanin.

phenomenon was observed by Wu et al. [58] in the LBG/PVA blend film. The L2 exhibits good interaction and compatibility between the two polymers (UWF and LBG) and the BPF anthocyanin compound, likely due to hydrogen bonding between the carboxylate (C=O) groups of the protein (gluten) and the –OH groups of the polysaccharides, working in conjunction with water-soluble anthocyanin [32]. Clearly, the L2 film exhibited a good balance of physical and structural properties and has been chosen for application as a pH indicator film with immobilised BPF anthocyanin.

3.3. Application of L2 film indicator in monitoring the freshness of silver pomfret fish

3.3.1. Colour changes of BPF anthocyanin and L2 film

Based on Fig. 2A, the BPF anthocyanin displayed various colour responses after exposure to a wide pH range. The colour of the BPF anthocyanin turned red in a buffer with a pH of 1 and 2, which is a strong acid. Then, the colour of the BPF anthocyanin turned to purple at pH 3 and to deep blue at pH 4–6, which is slightly acidic. The natural pH 7 and 8 were displayed in blue. The colour of the BPF extract changed to bluish-green at pH 9 and 10, greenish at pH 11, dark green at pH 12, and yellow at pH 13 in alkaline conditions. These colour changes were

similar to those reported in the previous study by Ahmad et al. [5].

The colour changes that happened were influenced by the shifting of the pH between H+ and OH- ions. The colour of anthocyanin at acidic pH values (pH < 2) was red, where the formation of the flavylium cation is favoured. This condition is fully protonated and has a delocalised H+ positive charge [56]. The first deprotonation occurred when a slight increase in pH, related to the kinetic reaction on acidic hydroxyl groups [9], favoured the colour change from red to purple and the formation of a quinoidal base. Further deprotonation occurred at pH values between 4 and 6, forming an anionic quinoidal base, which resulted in a colour change from purple to blue. After that, the stability of anthocyanins gradually declines as pH increases (pH > 7), causing a colour change from green to yellow in alkaline conditions. This results from the addition of OH- ion and isomerisation into chalcone formation [50]. Due to these abilities (colour changes), BPF anthocyanin could be beneficial for developing intelligent packaging to monitor the freshness of food products, which is associated with a rise in pH.

L2 film, identified from preliminary research, was chosen as a pH indicator film due to its good mechanical and water barrier properties. Based on Fig. 2B, the colour trend of L2 films corresponded to the BPF anthocyanin extract (Fig. 2A) where the colour gradually changed from red (pH 1) to pink (pH 2) to purple (pH 3) to blue (pH 4–5) to deep blue (pH 6) to bluish green (pH 7–9) to greenish (pH 10–11) to darken green (pH 12) and yellow (pH 13). A previous study reported similar colour changes from red to yellow in semolina agar starch films incorporated with BPF after being immersed in pH levels ranging from 1 to 13, indicating that the films exhibit a prominent colour response to different pH values [51]. Thus, the results showed that BPF anthocyanin had excellent colour stability when reacting with various pH solutions. The colour changes of the LBG:UWF pH indicator films can be effective for their application in monitoring the freshness of food products.

3.3.2. Colour stability and light barrier properties of L2 film

Fig. 3 shows the L2 film's colour stability (ΔE) and light barrier properties (opacity) change over 9 days of storage at room (25°C), chiller (4°C), and frozen (-18°C) temperatures. In Fig. 3A, the colour stability is represented by the ΔE values, which indicate the magnitude of colour change [33]. It is observed that at day 3, the ΔE values are relatively stable across all storage temperatures. However, from day 6 to day 9, there is a noticeable increase in ΔE , especially at the frozen temperature (9.75 \pm 0.56), indicating a highly significant change in colour under this condition. This colour change is attributed to structural stress in the polymer matrix, which affects anthocyanin stability and leads to greater colour degradation [19,47]. Besides, ΔE values are lowest at room temperature (4.99 \pm 0.11) and chiller temperature (7.95 \pm 0.81) during short storage, indicating better colour stability of anthocyanin pigments under these temperature conditions. Similar research was observed by Chen et al. [15] in corn wheat starch film.

The opacity of a film represents its ability to block or absorb light. For food packaging films, good light barrier properties protect the contents from harmful effects of light, such as photo-oxidation or pigment degradation [44]. Fig. 3B shows the variation in the opacity of the L2 film with time under different storage conditions. The opacity of the L2 film remained relatively unchanged with increasing storage time. However, over the nine days, the opacity decreases slightly at all temperatures, exhibiting a gradual decrease in opacity that indicates a loss of light barrier capacity over time. Chen et al. [15] reported similar findings, where the light barrier properties of bilayer films did not change significantly with prolonged storage.

3.3.3. Application of L2 film on silver pomfret fish

To determine the practicality of the L2 indicator in monitoring the freshness of silver pomfret fish, the L2 film was placed on top of the package, avoiding direct contact with the food items. Thus, the L2 film will only come into contact with volatile compounds released by the fish, providing direct information to the consumer with their naked eye.

Table 4
Surface and cross-section morphology of the pH indicator film with different ratios of LBG and UWF incorporated with BPF anthocyanin.

Film types	Upper Surface	Cross-section
L1	COS 20 gas (MUTATION P.C. SE VV 08.0, Segum Segum) Segu 08. 200 Segum	
U1	SED 10 0X Wp18mm P.C. 50 HV Vp1 99/m Sep 05, 2023	SED 16 DAY WOLFS IN D. P. A. B. C. B. C. A. B. B. C. A. B. C. B. C. A. B. C
LU	SEC 10.05 WOTHShim P.C.Se fry 1000 Marie Sept Del 2023	SED 16 Jan Wo Temmin C. 50 NV 1230 190 mm. EMUPM (JSM IT 169) Sep 0% 2023
L2	SED 10 0kV WD1fimm P.Ç.50 HV >x500 50µm Sep 05, 2023	SSID 16.0kV W015HmmR-C,50 HV , 1200 160µm Sep 66, 2023
U2	SED 16.8KV WD19mmP.C.50 HV x500 50µm Sep 95, 2023	SED 10.50V WD Immit P.C.50 4(V 2250 195)un 5. 560,8520337

The magnification used for surface and cross-section images is $500 \times .$ L1 = 100 LBG:0 UWF; U1 = 0 LBG: 100 UWF; LU = 50 LBG: 50 UWF; L2 = 70 LBG: 30 UWF; U2 = 30 LBG: 70 UWF.

Parameters related to the freshness of silver pomfret and the colour value of the L2 film indicator are presented in Fig. 4. The initial pH of silver pomfret was 7.10 \pm 0.10 (Fig. 4A), which increased with the storage time. At the end of the storage period, the pH of the silver pomfret increased to 8.16 \pm 0.06. This pH increase was attributed to the

accumulation of volatile basic nitrogen (NH $_3$), resulting from protein breakdown caused by microbial activity [46]. This finding is similar to previous studies by Boonsiriwit et al. [10].

Other than that, the initial colour of the L2 indicator was used as a reference for ΔE calculation, and changes in ΔE during storage are

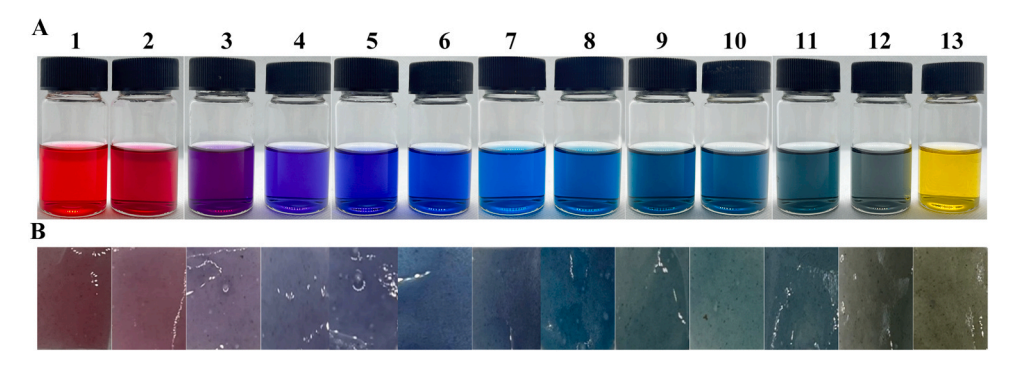
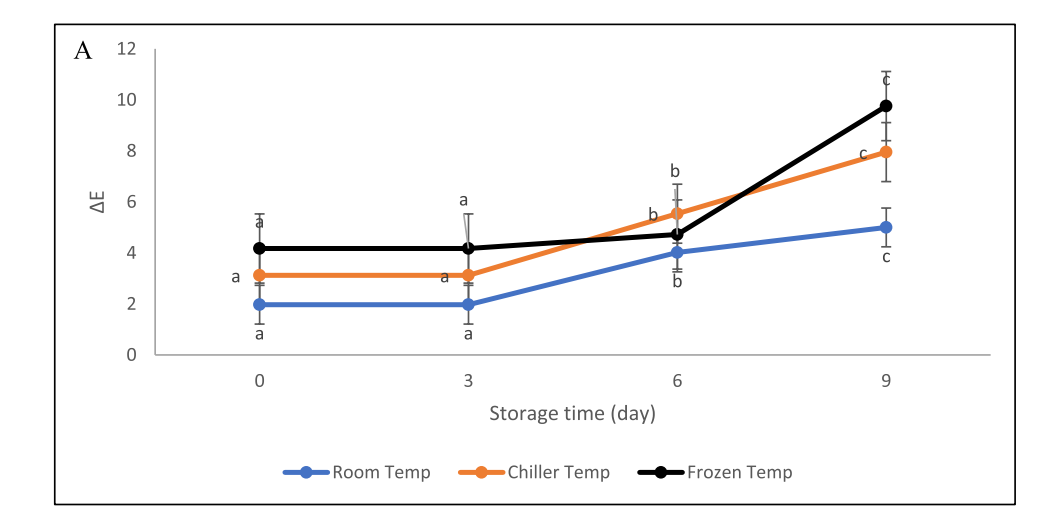


Fig. 2. Colour changes of BPF anthocyanin (A) and LBG/UWF (L2) film matrix (B) in different pH buffer solutions (pH 1.0-13.0).



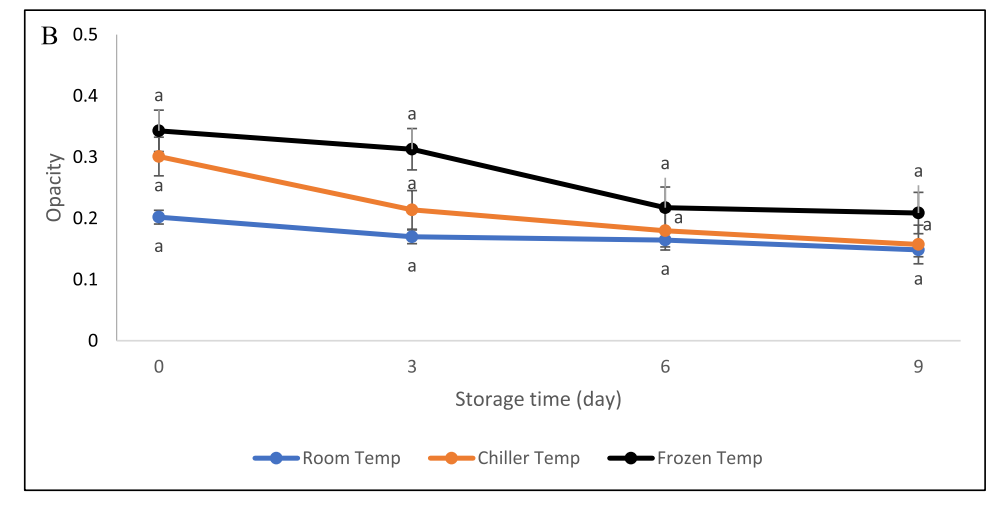
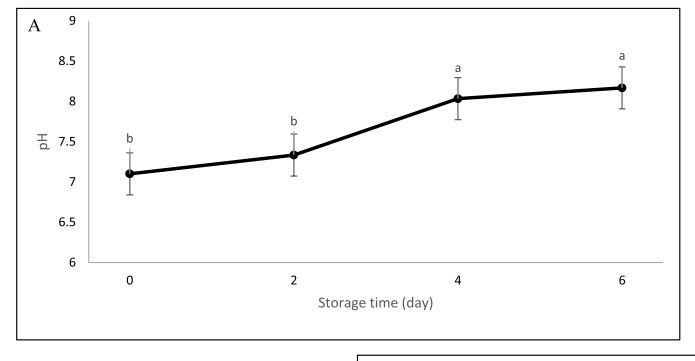
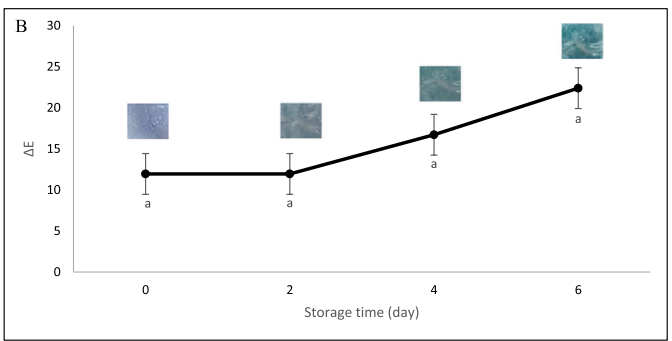


Fig. 3. Colour stability (A) and light barrier (B) properties of L2 film during storage at three different temperatures.

presented in Fig. 4B. The ΔE value after 2 days of storage was 11.94 \pm 3.60, which increased with an increase in spoilage parameters. The ΔE value of the L2 indicator increased sharply to 22.38 \pm 3.57 after 6 days of storage, and the indicator changed from blue to a greenish blue. Thus, the colour of the L2 indicator changed according to the changes in the quality of silver pomfret. Therefore, the silver pomfret was marked as spoiled after 4 days of storage. Images of fish packaging and changes in the colour of the L2 indicator are presented in Fig. 4C. Initially, the indicator was deep blue (fresh), which turned to light blue (fresh), greenish blue (spoiled), and green (spoiled) after 0, 2, 4, and 6 days of storage, respectively.

The appearance of the L2 indicator changed from blue to green over time due to the absorption of moisture and volatile nitrogen from the packaging headspace. Previous studies have shown that microbial activity in fish releases volatile basic nitrogenous compounds (TVB-N), primarily trimethylamine (TMA) and dimethylamine (DMA), which increase the pH during storage and indicate spoilage [12]. TMA, a natural marine compound with a strong fishy odour, accumulates in spoiled silver pomfret, raising the sample's pH to an alkaline condition [17]. This rise in alkaline volatile amines increases hydroxide ions (OH-), which convert BPF's anthocyanin into a carbinol base [2], causing the L2 indicator to change from blue to green colour. Therefore, the L2





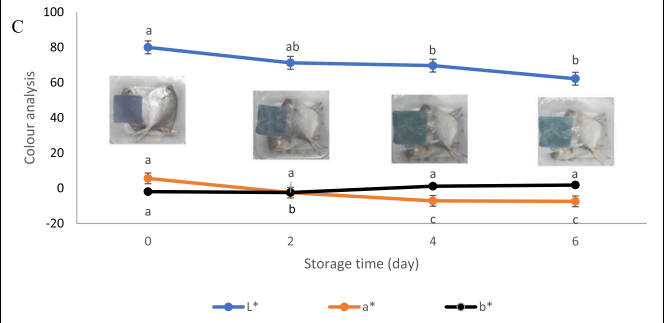


Fig. 4. pH of silver pomfret (A), colour change (ΔE) of the L2 film indicator (B), and L^* , a^* , b^* values of the L2 film on silver pomfret packages (C) during storage at 4°C.

indicator was selected to monitor the freshness of silver pomfret due to its ability to change colour on each sampling day clearly. This study highlights the potential of pH-sensitive indicators for detecting spoilage gases in intelligent packaging.

4. Conclusion

Films containing LBG demonstrated greater stability than those with UWF. However, the pure LBG film (L1) displayed high swelling properties, water solubility, and low elongation at break, which limits the functionality of LBG as a pH indicator film. Conversely, UWF films exhibited superior tensile and water resistance properties. The combination of LBG and UWF in various ratios enhanced the mechanical, water barrier, and structural properties of the films, making them more suitable for use as pH indicator films. The optimal formulation comprised 70 % LBG and 30 % UWF (L2), resulting in a stable film with low moisture content, the greatest thickness, strong water vapour permeability (WVP), high tensile strength, good elongation at break (EB), and compact structure in SEM compared to other composite films. The L2 indicator showed clear colour changes corresponding to the quality deterioration of silver pomfret. The release of alkaline compounds increased the pH, which altered the BPF anthocyanins and caused the L2 film to shift from blue (fresh) to green (spoiled) colour. Therefore, the blend of polymers between LBG and UWF (L2) proved to be the most suitable for developing an intelligent pH indicator. These findings offer valuable insights for further research on the application of pH indicators to monitor the freshness of muscle food products.

CRediT authorship contribution statement

Nur Nabilah Hasanah: Writing – original draft, Methodology, Investigation, Formal analysis, Data curation. Ezzat Mohamad Azman: Supervision, Writing - review & editing, Resources, Methodology, Validation. Ashari Rozzamri: Supervision, Writing - review & editing. Nur Hanani Zainal Abedin: Supervision, Writing - review & editing. Mohammad Rashedi Ismail-Fitry: Supervision, Project administration, Funding acquisition, Conceptualisation, Writing - review & editing.

Declaration of Competing Interest

The authors declare the following financial interests/personal relationships, which may be considered as potential competing interests: Mohammad Rashedi Ismail-Fitry reports that financial support was provided by the Ministry of Higher Education. For other authors, they declare that they have no known competing financial interests or personal relationships that could have appeared to influence the work reported in this paper.

Acknowledgements

This research was funded by the Malaysian Ministry of Higher Education, grant number FRGS/1/2020/WAB04/UPM/01/3.

References

- [1] R. Abedi-Firoozjah, S. Yousefi, M. Heydari, F. Seyedfatehi, S. Jafarzadeh, R. Mohammadi, F. Garavand, Application of red cabbage anthocyanins as pHsensitive pigments in smart food packaging and sensors, Polymers 14 (8) (2022) 1629.
- [2] K. Abhari, H. Hosseini, Enzymes in meat, fish, and poultry products processing and preservation-I, Nov. Food Grade Enzym. Appl. Food Process. Preserv. Ind. (2022) 183–191.
- [3] A.N. Adilah, B. Jamilah, M.A. Noranizan, Z.N. Hanani, Utilization of mango peel extracts on the biodegradable films for active packaging, Food Packag. Shelf Life 16 (2018) 1–7.
- [4] A.N. Ahmad, S. Abdullah Lim, N. Navaranjan, Development of sago (Metroxylon sagu)-based colorimetric indicator incorporated with butterfly pea (clitoria ternatea) anthocyanin for intelligent food packaging, J. Food Saf. 40 (4) (2020) e12807
- [5] S.N.S.S. Ahmad, N.N. Hasanah, M.R. Ismail-Fitry, Butterfly pea flower-infused quinoa starch film as a ph indicator for shellfish freshness assessment, Malays. J. Anal. Sci. (2024).
- [6] J.M. Alvarez-Suarez, C. Cuadrado, I.B. Redondo, F. Giampieri, A.M. González-Paramás, C. Santos-Buelga, Novel approaches in anthocyanin research-Plant fortification and bioavailability issues, Trends Food Sci. Technol. 117 (2021) 02 105
- [7] Bailey, N. (2023, February 2). The real difference between bleached and unbleached flour. Tasting Table. (https://www.tastingtable.com/1109562/the-real-differen ce-between-bleached-and-unbleached-flour/).
- [8] S. Barak, D. Mudgil, Locust bean gum: processing, properties and food applications—A review, Int. J. Biol. Macromol. 66 (2014) 74–80.

- [9] N. Basílio, F. Pina, Chemistry and photochemistry of anthocyanins and related compounds: a thermodynamic and kinetic approach, Molecules 21 (2016) 1502.
- [10] A. Boonsiriwit, M. Lee, M. Kim, P. Inthamat, U. Siripatrawan, Y.S. Lee, Hydroxypropyl methylcellulose/microcrystalline cellulose biocomposite film incorporated with butterfly pea anthocyanin as a sustainable pH-responsive indicator for intelligent food-packaging applications, Food Biosci. 44 (2021) 101392
- [11] Campbell, S.M., Pearson, B., & Marble, S.C. (2019). Butterfly pea (Clitoria ternatea) flower extract (BPFE) and Its use as a pH-dependent natural colorant: (ENH-1309/ EP573. 4/2019). EDIS. 2019(2).
- [12] P. Castro, J.C.P. Padrón, M.J.C. Cansino, E.S. Velázquez, R.M. De Larriva, Total volatile base nitrogen and its use to assess freshness in european sea bass stored in ice, Food Control 17 (4) (2006) 245–248.
- [13] P. Cazón, G. Velazquez, J.A. Ramírez, M. Vázquez, Polysaccharide-based films and coatings for food packaging: a review, Food Hydrocoll. 68 (2017) 136–148.
- [14] S. Chen, S. Brahma, J. Mackay, C. Cao, B. Aliakbarian, The role of smart packaging system in food supply chain, J. Food Sci. 85 (3) (2020) 517–525.
- [15] C. Chen, Y. Du, G. Zuo, F. Chen, K. Liu, L. Zhang, Effect of storage condition on the physico-chemical properties of corn—wheat starch/zein edible bilayer films, R. Soc. Open Sci. 7 (2) (2020) 191777.
- [16] H. Cheng, H. Xu, D.J. McClements, L. Chen, A. Jiao, Y. Tian, Z. Jin, Recent advances in intelligent food packaging materials: principles, preparation and applications, Food Chem. 375 (2022) 131738.
- [17] J. Das, H.N. Mishra, A comprehensive review of the spoilage of shrimp and advances in various indicators/sensors for shrimp spoilage monitoring, Food Res. Int. 173 (2023) 113270.
- [18] S. Dayang, M. Irwanto, N. Gomesh, Nature based dyes from blue pea flower as a potential sensitizer for dssc, J. Eng. Res. Educ. 8 (2016) 59–66.
- [19] P.K. Dutta, D. Hui, Low-temperature and freeze-thaw durability of thick composites, Composites Part B Engineering 27 (3-4) (1996) 371–379.
- [20] K.Y. Ee, M.K. Eng, M.L. Lee, Physicochemical, thermal and rheological properties of commercial wheat flours and corresponding starches, Food Sci. Technol. 40 (2020) 51–59.
- [21] J.L. Fan, N. Han, H.Q. Chen, Physicochemical and structural properties of wheat gluten/rice starch dough-like model, J. Cereal Sci. 98 (2021) 103181.
- [22] G. Ghoshal, Recent trends in active, smart, and intelligent packaging for food products. In Food Packaging and Preservation, Academic Press, 2018, pp. 343–374.
- [23] B. Gieroba, A. Sroka-Bartnicka, P. Kazimierczak, G. Kalisz, A. Lewalska-Graczyk, V. Vivcharenko, A. Przekora, Surface chemical and morphological analysis of chitosan/1, 3-β-d-glucan polysaccharide films cross-linked at 90° c, Int. J. Mol. Sci. 23 (11) (2022) 5953.
- [24] H. Goesaert, K. Brijs, W.S. Veraverbeke, C.M. Courtin, K. Gebruers, J.A. Delcour, Wheat flour constituents: how they impact bread quality, and how to impact their functionality, Trends Food Sci. Technol. 16 (1–3) (2005) 12–30.
- [25] Z.N. Hanani, Y.H. Roos, J.P. Kerry, Use of beef, pork and fish gelatine sources in the manufacture of films and assessment of their composition and mechanical properties, Food Hydrocoll. 29 (1) (2012) 144–151.
- [26] N.N. Hasanah, E. Mohamad Azman, A. Rozzamri, N.H. Zainal Abedin, M.R. Ismail-Fitry, A systematic review of butterfly pea flower (clitoria ternatea l.): extraction and application as a food freshness pH-indicator for polymer-based intelligent packaging, Polymers 15 (11) (2023) 2541.
- [27] S.B. Hashim, H.E. Tahir, L. Liu, J. Zhang, X. Zhai, A.A. Mahdi, S. Jiyong, Intelligent colorimetric ph sensoring packaging films based on sugarcane wax/agar integrated with butterfly pea flower extract for optical tracking of shrimp freshness, Food Chem. 373 (2022) 131514
- [28] N.J. Hirpara, M.N. Dabhi, A review on effect of amylose/amylopectin, lipid and relative humidity on starch based biodegradable films, Int. J. Curr. Microbiol. Appl. Sci. 10 (4) (2021) 500–531.
- [29] H. Hu, M. Qiu, Z. Qiu, S. Li, L. Lan, X. Liu, Variation in wheat quality and starch structure under granary conditions during long-term storage, Foods 12 (9) (2023) 1886
- [30] N. Husin, M.Z.A. Rahim, M. Zulkhairi, M. Azizan, M.A. Mohd Noor, M. Rashedi, M. R. Ismail-Fitry, N. Hassan, Real-time monitoring of food freshness using delphinidin-based visual, Malays. J. Anal. Sci. 24 (2020) 558–569.
- [31] Y.F. Jiang, Y.X. Li, Z. Chai, X.J. Leng, Study of the physical properties of whey protein isolate and gelatin composite films, J. Agric. Food Chem. 58 (2010) 5100–5108.
- [32] R.R. Koshy, A. Reghunadhan, S.K. Mary, P.S. Pillai, S. Joseph, L.A. Pothen, Ph indicator films fabricated from soy protein isolate modified with chitin nanowhisker and clitoria ternatea flower extract, Curr. Res. Food Sci. 5 (2022) 743–751.
- [33] Y.K. Lee, Comparison of CIELAB ΔE* and CIEDE2000 color-differences after polymerization and thermocycling of resin composites, Dent. Mater. 21 (7) (2005) 678–682.
- [34] M. Li, C. Liu, X. Zheng, J. Hong, K. Bian, L. Li, Interaction between A-type/B-type starch granules and gluten in dough during mixing, Food Chem. 358 (2021) 120870
- [35] F. Liu, W. Chang, M. Chen, F. Xu, J. Ma, F. Zhong, Film-forming properties of guar gum, tara gum and locust bean gum, Food Hydrocoll. 98 (2020) 105007.
- [36] J. Long, W. Zhang, M. Zhao, C.Q. Ruan, The reduce of water vapor permeability of polysaccharide-based films in food packaging: a comprehensive review, Carbohydr. Polym. 321 (2023) 121267.
- [37] K. Mahmood, H. Kamilah, P.L. Shang, S. Sulaiman, F. Ariffin, A.K. Alias, A review: interaction of starch/non-starch hydrocolloid blending and the recent food applications, Food Biosci. 19 (2017) 110–120.

[38] J.T. Martins, M.A. Cerqueira, A.I. Bourbon, A.C. Pinheiro, B.W.S. Souza, A. A. Vicente, Synergistic effects between κ-carrageenan and locust bean gum on physicochemical properties of edible films made thereof, Food Hydrocoll. 29 (2) (2012) 280–289.

- [39] S.K. Mary, R.R. Koshy, J. Daniel, J.T. Koshy, L.A. Pothen, S. Thomas, Development of starch based intelligent films by incorporating anthocyanins of butterfly pea flower and TiO₂ and their applicability as freshness sensors for prawns during storage, RSC Adv. 10 (65) (2020) 39822–39830.
- [40] Z.A. Maryam Adilah, B. Jamilah, Z.A. Nur Hanani, Functional and antioxidant properties of protein-based films incorporated with mango kernel extract for active packaging, Food Hydrocoll. 74 (2018) 207–218.
- [41] Mitchell, P. (2011, July 8). What is the pH level of flour? Livestrong.com. (https://www.livestrong.com/article/486762-what-is-the-ph-lev el-of-flour/#google_vignette).
- [42] G.W. Monier-Williams, On the chemical changes produced in flour by bleaching, Epidemiol. Infect. 11 (2) (1911) 167–187.
- [43] F.S. Mostafavi, R. Kadkhodaee, B. Emadzadeh, A. Koocheki, Preparation and characterization of tragacanth-locust bean gum edible blend films, Carbohydr. Polym. 139 (2016) 20–27.
- [44] M. Mujtaba, J. Lipponen, M. Ojanen, S. Puttonen, H. Vaittinen, Trends and challenges in the development of bio-based barrier coating materials for paper/ cardboard food packaging; a review, Sci. Total Environ. 851 (2022) 158328.
- [45] J. Peralta, C.M. Bitencourt-Cervi, V.B. Maciel, C.M. Yoshida, R.A. Carvalho, Aqueous hibiscus extract as a potential natural pH indicator incorporated in natural polymeric films, Food Packag. Shelf Life 19 (2019) 47–55.
- [46] Z. Ramezani, M. Zarei, N. Raminnejad, Comparing the effectiveness of chitosan and nanochitosan coatings on the quality of refrigerated silver carp fillets, Food Control 51 (2015) 43–48.
- [47] O. Romruen, P. Kaewprachu, S. Sai-Ut, P. Kingwascharapong, T. Karbowiak, W. Zhang, S. Rawdkuen, Impact of environmental storage conditions on properties and stability of a smart bilayer film, Sci. Rep. 14 (1) (2024) 23038.
- [48] S. Sai-Ut, P. Suthiluk, W. Tongdeesoontorn, S. Rawdkuen, P. Kaewprachu, T. Karbowiak, P. Degraeve, Using anthocyanin extracts from butterfly pea as ph indicator for intelligent gelatin film and methylcellulose film, Curr. Appl. Sci. Technol. (2021) 652–661.
- [49] L.G. Santos, V.G. Martins, Optimization of the Green extraction of polyphenols from the edible flower clitoria ternatea by high-power ultrasound: a comparative study with conventional extraction techniques, J. Appl. Res. Med. Aromat. Plants 34 (2023) 100458.
- [50] N.M. Saptarini, D. Suryasaputra, H. Nurmalia, Application of butterfly pea (clitoria ternatea Linn) extract as an indicator of acid-base titration, J. Chem. Pharm. Res. 7 (2015) 275–280.
- [51] S. Saravanan, N.A. Abdullah, N.N. Hasanah, E.M. Azman, N.H.Z. Abedin, M. R. Ismail-Fitry, Development of semolina starch/agar-based intelligent films by incorporating butterfly pea flower anthocyanins to monitor the freshness of prawns, Sains Malays. 53 (1) (2024) 87–98.
- [52] R.S. Singh, N. Kaur, V. Rana, R.K. Singla, N. Kang, G. Kaur, H. Kaur, J.F. Kennedy, Carbamoylethyl locust bean gum: synthesis, characterization and evaluation of its film forming potential, Int. J. Biol. Macromol. 149 (2020) 348–358.
- [53] S.N. Syahida, M.R. Ismail-Fitry, Z.M.A. Ainun, Z.A.N. Hanani, Effects of gelatin/ palm wax/lemongrass essential oil (GPL)-coated kraft paper on the quality and shelf life of ground beef stored at 4°C, Food Packag. Shelf Life 28 (2021) 100640.
- [54] J. Wang, X. Sun, X. Xu, Q. Sun, M. Li, Y. Wang, F. Xie, Wheat flour-based edible films: effect of gluten on the rheological properties, structure, and film characteristics, Int. J. Mol. Sci. 23 (19) (2022) 11668.
- [55] R. Welc-Stanowska, K. Kłosok, A. Nawrocka, Insight into organization of gliadin and glutenin extracted from gluten modified by phenolic acids, Molecules 28 (23) (2023) 7790.
- [56] B. Wiyantoko, Butterfly pea (*clitoria ternatea* L.) extract as indicator of acid-base titration, Indones. J. Chem. Anal. 3 (1) (2020) 22–32.
- [57] B. Wiyantoko, A. Astuti, Butterfly Pea (*Clitoria Ternatea* L.) extract as indicator of acid-base titration, Indones, J. Chem. Anal. 3 (1) (2020) 22–32.
- [58] Y. Wu, P. Tang, S. Quan, H. Zhang, K. Wang, J. Liu, Preparation, characterization and application of smart packaging films based on locust bean gum/polyvinyl alcohol blend and betacyanins from cockscomb (celosia cristata L.) flower, Int. J. Biol. Macromol. 191 (2021) 679–688.
- [59] J. Xu, Y. Li, Wheat gluten-based coatings and films: preparation, properties, and applications, J. Food Sci. 88 (2) (2023) 582–594.
- [60] F. Xue, M. Zhao, X. Liu, R. Chu, Z. Qiao, C. Li, B. Adhikari, Physicochemical properties of chitosan/zein/essential oil emulsion-based active films functionalized by polyphenols, Future Foods 3 (2021) 100033.
- [61] X. Yao, J. Liu, H. Hu, D. Yun, J. Liu, Development and comparison of different polysaccharide/PVA-based active/intelligent packaging films containing red pitaya betacyanins, Food Hydrocoll. 124 (2022) 107305.
- [62] H. Yong, J. Liu, J. Kan, J. Liu, Active/intelligent packaging films developed by immobilizing anthocyanins from purple sweetpotato nd purple cabbage in locust bean gum, chitosan and κ-carrageenan-based matrices, Int. J. Biol. Macromol. 211 (2022) 238–248.
- [63] E. Young, M. Mirosa, P. Bremer, A systematic review of consumer perceptions of smart packaging technologies for food, Front. Sustain. Food Syst. 4 (2020) 63.
- [64] L. Yuan, Y. Wu, Y. Qin, H. Yong, J. Liu, Recent advances in the preparation, characterization and applications of locust bean gum-based films, J. Renew. Mater. 8 (12) (2020) 1565–1579.
- [65] D. Yun, Y. He, H. Zhu, Y. Hui, C. Li, D. Chen, J. Liu, Smart packaging films based on locust bean gum, polyvinyl alcohol, the crude extract of loropetalum chinense var.

- $\it rubrum$ petals and its purified fractions, Int. J. Biol. Macromol. 205 (2022) 141–153.
- [66] X. Zhai, J. Shi, X. Zou, S. Wang, C. Jiang, J. Zhang, Novel colorimetric films based on starch/polyvinyl alcohol incorporated with roselle anthocyanins for fish freshness monitoring, Food Hydrocoll. 69 (2017) 308–317.
- [67] L. Zheng, L. Liu, J. Yu, P. Shao, Novel trends and applications of natural pHresponsive indicator film in food packaging for improved quality monitoring, Food Control 134 (2022) 108769.
- Control 134 (2022) 108769.

 [68] B.J. Zhu, M.Z. Zayed, H.X. Zhu, J. Zhao, S.P. Li, Functional polysaccharides of carob fruit: a review, Chin. Med. 14 (1) (2019) 40.